



ELSEVIER

Physica A 249 (1998) 10–17

PHYSICA A

# Propagating solitary states in highly dissipative driven fluids

J. Fineberg\*, O. Lioubashevski

*The Racah Institute of Physics, The Hebrew University of Jerusalem, Jerusalem 91904, Israel*

---

## Abstract

Highly localized solitary states, driven by means of the spatially uniform, vertical acceleration of a thin fluid layer, are observed to propagate along the 2D surface of a fluid in a highly dissipative regime. Unlike classical solitons, these states propagate at a single constant velocity for given fluid parameters and their existence is dependent on the highly dissipative character of the system. The properties of these states are discussed and examples of bound states and two-state interactions are presented. © 1998 Elsevier Science B.V. All rights reserved.

---

Highly localized states have long captured the imagination of Physicists in disciplines ranging from solid state to high-energy physics. Non-linear systems, in particular, have an inherent ability for self-organization or self-focusing that, in many cases, gives rise to these intriguing states. A classic example is the soliton, first documented by Russell [1], as he chased it on horseback through the canals of 19th century Scotland. Soliton-type structures have since been observed in a wide class of conservative or nearly conservative non-linear systems where the balance between non-linear amplification and dispersion can give rise to stable, highly localized structures. We now pose the question of whether these types of structures can exist in dissipative systems. Localized, soliton-like structures, ubiquitous in 1D non-linear integrable systems, are rarely if at all observed in highly dissipative 2D or 3D systems. Recent studies of 1D classical conservative systems show that dissipation strongly influences solitons. In extensions of the Kuramoto–Sivashinsky (KS) and KdV equations [2], although soliton-like solutions were seen to persist, the addition of slight dissipative effects was enough to cause the collapse of a family of solitons having a continuum of propagation velocities to a single selected state. Highly localized soliton-like states have also been observed as stable solutions of dissipative subcritical complex Ginzburg–Landau equations with fifth-order damping terms. In these 2D systems both stationary [3] and

---

\* Corresponding author.

breathing solutions [4] were observed. Study of two-state interactions between the latter states revealed a strong dependence of the interaction product on the relative phase of the interacting states.

There have been a number of recent experimental observations of localized propagating states in 2D dissipative systems. Temporally, intermittent localized structures have been observed in the convection of binary mixtures [5,6] and localized states which, upon collision, can either annihilate or pass through each other have been seen in the catalytic oxidation of CO on a 2D substrate [7]. Recent experiments [8,9] have revealed highly localized propagating solitary structures upon the spatially uniform, vertical acceleration of a thin fluid layer of viscous fluid. Surprisingly, strikingly similar structures [10] were later observed when a granular medium was excited in the same way.

The latter two experiments were especially significant in that the solitary states occurred in systems which are *highly* dissipative. In contrast to classical solitons which tend to be destroyed upon the introduction of dissipation, we shall see that in the case of a viscous fluid, the highly dissipative nature of the system is *necessary* for the formation of these states. Thus, we might be looking at a new type of non-linear phenomena – highly localized states where dissipation plays a key role in their formation and stability. Below, after a description of the experimental system, we will describe some of the properties of these intriguing states and present examples of their mutual interactions. Finally, we will mention some recent work in the scaling behavior of the linear threshold of the system that indicates that, in the highly dissipative regime, a Rayleigh–Taylor-type mechanism is the dominant mechanism for instability.

Our experimental system is similar to those generally used to study the well-known Faraday instability, which generates parametrically driven surface waves. We subject a featureless layer of fluid to uniform, externally imposed oscillations in the vertical (parallel to gravity) direction. The acceleration,  $a$ , of the fluid layer can be viewed as the system's control parameter. At a critical value of the layer acceleration,  $a_c$ , a bifurcation occurs to parametric waves on the fluid surface which oscillate at half of the external driving frequency. Solitary states then spontaneously appear at well-defined values of  $a$ , typically a few percent above  $a_c$ . The system is further characterized by the quantities  $\omega$ ,  $h$ ,  $\nu$ ,  $\rho$ , and  $\sigma$  defined as the externally imposed angular frequency, depth of the fluid layer, kinematic viscosity, fluid density and surface tension, respectively. As previously described in Refs. [8,9], our experiments were performed in a 144.0 mm diameter circular cell with the fluid supported by an aluminum plate, polished to a mirror surface and flat to  $1\ \mu\text{m}$ . The cell's lateral boundaries, made of Delrin, were sloped at a  $20^\circ$  angle to reduce meniscus formation on the fluid surface. The fluid depth varied between 1.0 and 5.0 mm. Fluids used were glycerol–water mixtures and the hydrocarbon flushing fluids, TKO–FF (described at length in Refs. [8,9]) and TKO–77. The fluid temperature was regulated to within  $0.01^\circ\text{C}$ . In the latter fluids  $\sigma$  and  $\nu$  were varied between 29.6 and 31.0 dyne/cm and from 4.7 to 0.25 St, respectively, as the temperature was varied over a  $20\text{--}45^\circ\text{C}$  range. The cell was mounted on a mechanical shaker providing vertical acceleration from 0 to  $30\ \text{g}$ 's over a frequency range of

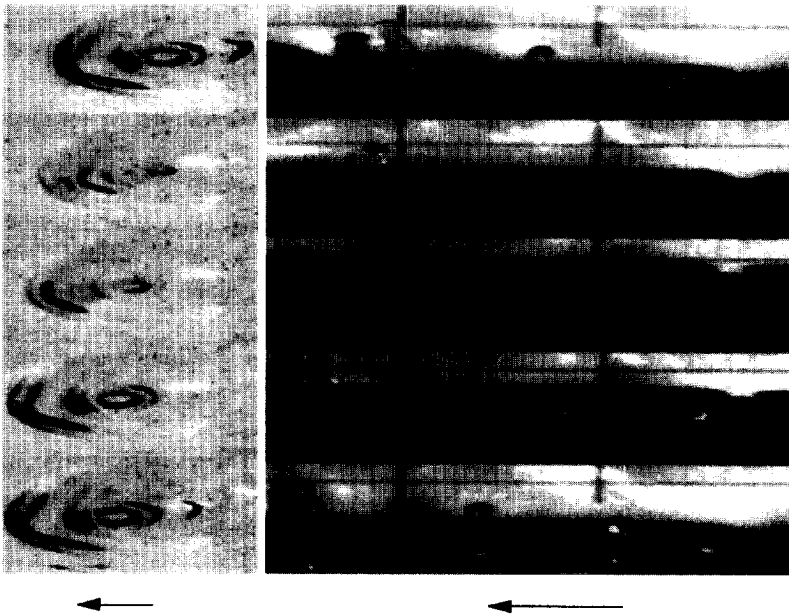


Fig. 1. Views from above (left) and the side (right) of typical propagating solitary states. One excitation period is shown where time increases from top to bottom and with a time interval of 8 ms between frames. Both the propagation and complex structure of the state as a function of the phase relative to the excitation is apparent. The arrows, indicating the propagation direction, are of length 1.5 cm.

20–80 Hz. The acceleration, monitored by a calibrated accelerometer, was regulated to within 0.01 g. To determine the instability onset, the system was visualized from above by shadowgraph with stroboscopic illumination. Direct visualization of the system was performed by scattered stroboscopic light viewed either from the side and above. Visualization was performed at rates of up to 360 Hz using a high-speed CCD camera [11].

Most previous experiments in this system were performed in the low  $v$ , large  $h$  limit ( $\lambda \ll h$  where  $\lambda$  is the wavelength of the excited pattern) at low dissipation (i.e. a dissipation rate  $\sim v/\lambda^2 \ll \omega$ ). These studies include non-linear mode interactions [12–14] in small aspect ratio systems, where the excited modes are well separated, and the dynamics and disorder of patterns [15–19] in larger aspect ratio systems. High  $v$  fluids in small  $h$  systems were recently introduced [20–22] to both reduce mode quantization effects and damp out long wavelength modes (for a detailed discussion see Ref. [21]). As we will see, this regime of high dissipation leads to new non-linear phenomena.

Typical views of the solitary state both from the side and above are presented in Fig. 1. As viewed from above, these states are similar in appearance to the “oscillon” states recently observed in granular media [10]. This state is hysteretic and large amplitude states spontaneously appear in the near vicinity of the system’s primary instability to spatially confined periodic states. For sufficiently large perturbations (e.g. mechanically striking the fluid layer) solitary states can be excited prior to the onset

of the confined pattern. The state has a non-trivial periodic temporal behavior (a single period is shown) with the same period as the forcing frequency,  $\omega$ . As in the dissipative extensions to the KdV and KS equations [2], for a given value of  $\omega$  a single constant-propagation velocity,  $v$ , is observed that is independent of the driving amplitude. Compared to the linear group velocity,  $v_g$ , of surface waves, the functional dependence of  $v$  is quite different. Although its basic scale is similar to  $v_g$ ,  $v$  varies only slightly as  $\omega$  is changed. Upon formation, these states are stable and can propagate in any direction. When guided by the lateral wall of the apparatus, single solitary states have been observed to propagate indefinitely around the circumference of the cell. Solitary states, generated by either collisions or external perturbations to the system, can exist far from the system boundaries with no apparent difference in their form or properties relative to states that propagate adjacent to the cell boundaries. The main mechanism for the destruction of these states is by collision with either other solitary structures or the system's lateral boundaries.

How general are these states and why have they not been observed in previous experiments? For any given values of  $v$  and  $h$  no solitary states are observed above a critical value of  $\omega$ . A dimensionless number relating these quantities is the ratio of the boundary-layer thickness,  $\delta \equiv (v/\omega)^{1/2}$ , to  $h$ . We view a highly dissipative system as one where the characteristic time for dissipation,  $h^2/v$ , is on the order of the driving period,  $1/\omega$ . The ratio  $\delta/h$  (or, equivalently, the ratio between the forcing and dissipative time scales) determines the selection of the fluid state. Above a critical value [8,9],  $(\delta/h)_{crit} = 0.30$ , solitary states spontaneously appear. Below this value global patterns, as observed in previous studies [12–22] where  $0.03 < \delta/h < 0.27$ , are formed. The parameter  $(\delta/h)^{-2}$ , analogous to a Reynolds number of the flow, can be obtained by scaling [23] the externally forced Navier–Stokes equations by the length scale  $h$  and the time scale  $\omega^{-1}$ .  $(\delta/h)_{crit}$  occurs in the region where the forced oscillation of the fluid surface approaches critical damping (when the viscous and driving time scales are comparable). Thus, the existence of solitary states is crucially linked to the system dissipation. The value of  $(\delta/h)_{crit}$  underlines the qualitative difference between the dissipative states observed here and “trough” solitons [24–26] observed in the low-dissipation regime. These latter solitons, described by a non-linear Schrodinger equation, were observed in a nearly conservative, 1D system for  $\delta/h \sim 0.01$ , a value far below  $(\delta/h)_{crit}$ .

Fig. 2 demonstrates the scaling properties of the solitary states. We find that the width of the state, defined as the distance between consecutive “fingers” at their maximal amplitude, scales with the linear wavelength,  $\lambda$ , of the system. The maximal amplitude of the state, on the other hand, scales with the amplitude,  $a/\omega^2$ , of the forcing.

Solitary states can interact in a number of ways. The interaction potential between them appears to be short-ranged as no perceptible change in form occurs until two states are within a wavelength of each other. Two states will interact via collision, where an example is shown in Fig. 3. Unlike classical solitons, which interact via a phase shift, the results of a collision between two solitary states can result in either the two states passing through each other with a small change in amplitude, mutual

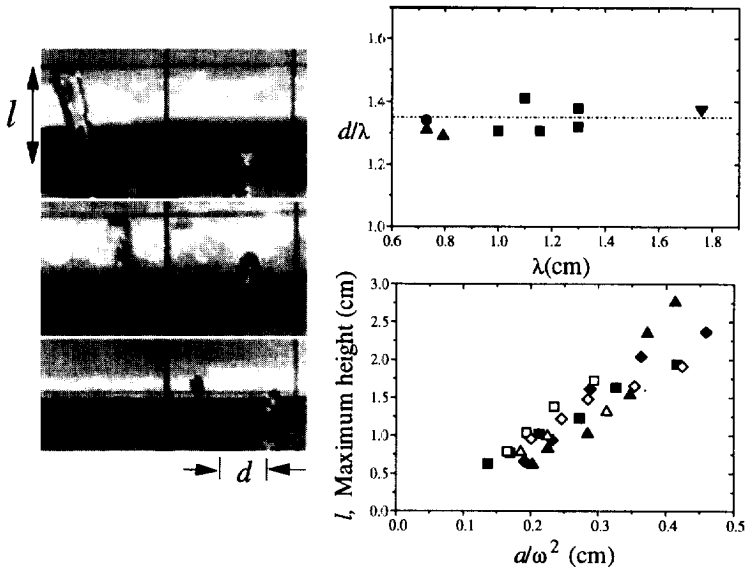


Fig. 2. Scaling of the solitary state. (Left) Transverse views at maximum amplitude for (top)  $\omega/2\pi = 20$  Hz,  $v = 1.4$  St.,  $h = 2.9$  mm; (center)  $\omega/2\pi = 26$  Hz,  $v = 1.25$  St.,  $h = 2.1$  mm (bottom)  $\omega/2\pi = 41$  Hz,  $v = 0.86$  St.,  $h = 1.0$  mm; (Right) the scaling of the width,  $d/\lambda$ , where  $d$  is distance between consecutive fingers and  $\lambda$  the wavelength of the primary instability (upper) and (lower) scaling of the height of the solitary states where  $l$  is the maximum amplitude of the state.

annihilation, or “billiard ball”-type collisions in which the resulting solitary state(s) leaves the collision region at a large angle relative to the axis described by the two initial states. An example of the latter type of collision is presented in Fig. 3, where a nearly “head-on” collision near the center of the cell resulted in the formation of two oppositely propagating states. One of these outgoing states was formed at a small amplitude and decayed as it propagated away from the collision site. The second state formed, propagating toward the bottom of the figure, was stable. This type of collision is reminiscent of simulations performed on dissipative solitary states formed within an interacting fifth-order Ginzburg–Landau-type model [4]. An interesting feature of collisions resulting in the formation of new states is that, as in interacting elementary particles, an intermediate “metastable” state is formed (Fig. 3 – center) which then decays into the final interaction products. In contrast to the initial and final states, this metastable state is non-propagating and exists for times longer than the time needed for a propagating state to traverse the interaction region.

Bound solitary states can also be formed, where typical two-state bound states are presented in Fig. 4. These states are formed by either collisions or initial conditions of the system and propagate with the same velocity as single solitary states. These states are weakly bound and can either spontaneously break up into a pair of single states or exist until perturbed by collision. Besides two-state bound states, other, generally unstable, multi-state bound states have been observed.



Fig. 3. A typical “head-on” collision of two solitary states which results in a “new” state. Note the formation of a metastable “bound” state upon collision.



Fig. 4. Typical view of two-state bound states, from the side (upper) and above (lower). Arrows indicate the propagation direction. When perturbed, these states become unstable to two single solitary states.

What is the mechanism for the formation of these states? A hint is suggested by the scaling behavior of the threshold for the linear stability of the system in this parameter regime. The first instability of the system is not to solitary states but to parametrically forced confined patterns with a typical example shown in Fig. 5a. The experimental

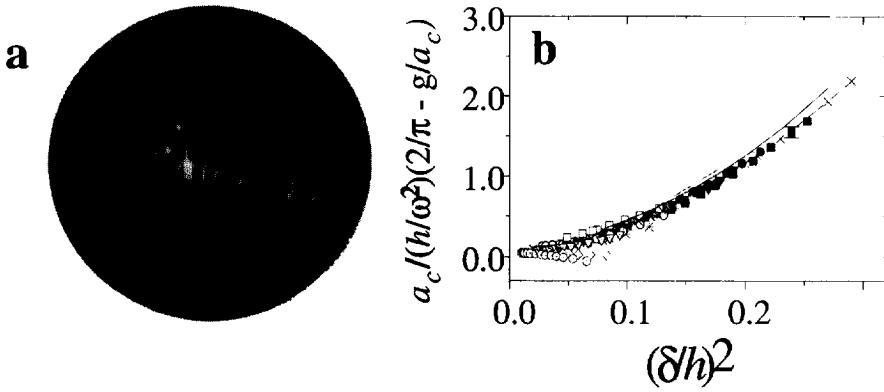


Fig. 5. (a) A typical example of the spatially confined primary instability of the system where  $\omega/2\pi = 42$  Hz,  $h = 1.0$  mm and  $\nu = 0.63$  St. (b) Scaling of reduced acceleration threshold,  $a_c/(h\omega^2)(2/\pi - g/a_c)$ , as a function of the dissipation parameter,  $(\delta/h)^2$ . Typically, over an order of magnitude in  $a_c$  is represented for each value of  $(\delta/h)^2$ . Experimental data ( $h$  in cm,  $\nu$  in St): (solid square)  $h = 0.1$ ,  $\nu = 0.58$ ; (solid triangle)  $h = 0.13$ ,  $\nu = 0.58$ ; (■)  $h = 0.13$ ,  $\nu = 0.8$ ; (solid inverted triangle)  $h = 0.15$ ,  $\nu = 0.8$ ; (solid diamond)  $h = 0.15$ ,  $\nu = 0.48$ ; (+)  $h = 0.21$ ,  $\nu = 0.8$ ; (×)  $h = 0.21$ ,  $\nu = 1.23$ ; (\*)  $h = 0.24$ ,  $\nu = 0.8$ ; (○)  $h = 0.3$ ,  $\nu = 1.23$ ; (open square)  $h = 0.51$ ,  $\nu = 2.53$ ; (dotted triangle)  $h = 0.21$ ,  $\nu = 0.48$ ; (dotted diamond)  $h = 0.25$ ,  $\nu = 0.41$ ; (dotted circles)  $h = 0.3$ ,  $\nu = 0.48$ . Numerical data: (dot-dashed line)  $h = 0.13$ ,  $\nu = 0.81$ ; (dashed line)  $h = 0.15$ ,  $\nu = 0.50$ ; (dotted line)  $h = 0.13$ ,  $\nu = 0.20$ . Note the following data sets where  $a_c < 2 - 3g$ : (dotted diamond)  $h = 0.25$  cm,  $\nu = 0.41$  St; and (dotted circles)  $h = 0.3$  cm,  $\nu = 0.48$  St. The solid line,  $A_{fit} = 0.059 + 21.46(\delta/h)^{3.54}$ , is a fit to the data. Representative error bars are shown.

system can be characterized by five dimensionless parameters that can be built using the seven quantities  $a$ ,  $\omega$ ,  $\nu$ ,  $\rho$ ,  $\sigma$ ,  $h$ ,  $L$ , along with the gravitational acceleration,  $g$ . With so many dimensionless parameters, there is no a priori reason to expect simple scaling behavior of the instability threshold to emerge. By combining experimental measurements and numerical calculations of the instability threshold with the Kumar–Tuckerman algorithm [27], we demonstrate (Fig. 5b) that, unexpectedly, in the highly dissipative high- $\nu$  low- $h$  regime, simple scaling of the critical acceleration indeed occurs in a surprisingly wide range of experimental parameters [23]. The scaling in this regime effectively reduces the dimension of parameter space from 5 to 2. The two dominant parameters that emerge are  $(\delta/h)^2$  which, as mentioned previously, determines the existence of solitary states, and a new parameter,  $a/(\omega^2 h)(2/\pi - g/a)$ . The acceleration difference  $(2a/\pi - g)$  that appears in this latter parameter suggests that a mechanism akin to the Rayleigh–Taylor instability may drive the instability in this regime. The Rayleigh–Taylor instability occurs when a dense fluid is accelerated into a less dense one (in our case air) and finger-like patterns of the denser fluid result. The numerical factor  $2/\pi$  accounts for the fact that  $a$  upwardly accelerates over only half of a cycle. The Faraday instability to parametrically driven surface waves can occur for values of  $a_c - g < 0$  and, as Fig. 5b shows, the breakdown of the scaling for these relatively low values of  $a$  suggests that the Faraday instability is a qualitatively different instability mechanism than that observed in the scaling regime.

In conclusion, we have described high-amplitude, highly localized solitary states that occur in a highly dissipative system. The conditions necessary for the formation of these states suggest that not only does dissipation not destroy these states, but that a high degree of dissipation may be *essential* for their existence. Intriguing questions regarding these states are their generality and the robustness of their characteristics. As mentioned above, a number of qualitatively similar type structures have recently been observed in experiments on a variety of driven non-linear systems and simulations of a number of dissipative model systems. If these “dissipative solitons” are indeed generic, what is their role in the dissipation and promotion of disorder in this and other nonlinear systems?

The authors wish to acknowledge the support of the Wolfson family charitable trust (Grant No. 43/93-2).

## References

- [1] J.S. Russell, Rep. 14th Meet. British Assoc. Adv. Sci., 1844, 311–390.
- [2] See, e.g., C.I. Christov, M.G. Velarde, *Physica D* 86 (1995) 323.
- [3] R.J. Deissler, H.R. Brand, *Phys. Rev. A* 44 (1991) 3411.
- [4] R.J. Deissler, H.R. Brand, *Phys. Rev. Lett.* 74 (1995) 4847.
- [5] V. Steinberg, J. Fineberg, E. Moses, I. Rehberg, *Physica D* 37 (1989) 359.
- [6] K. Lerman, E. Bodenschatz, D.S. Cannell, G. Ahlers, *Phys. Rev. Lett.* 70 (1993) 3572.
- [7] H.H. Rotermund, S. Jakubith, A. von Oertzen, G. Ertl, *Phys. Rev. Lett.* 66 (1991) 3083.
- [8] O. Lioubashevski, H. Arbel, J. Fineberg, *Phys. Rev. Lett.* 76 (1996) 3959.
- [9] J. Fineberg, *Nature* 382 (1996) 763.
- [10] P.B. Umbanhuar, F. Melo, H.L. Swinney, *Nature* 382 (1996) 793.
- [11] We used a JAI model CVM-30 camera interfaced to a Matrox Pulsar framegrabber.
- [12] See, e.g., J.P. Gollub, C.W. Meyer, *Physica D* 6 (1983) 337.
- [13] J.P. Gollub, S. Ciliberto, *Phys. Rev. Lett.* 52 (1985) 922.
- [14] F. Simonella, J.P. Gollub, *J. Fluid Mech.* 199 (1989) 471.
- [15] See e.g., A.B. Ezerskii, P.I. Korotin, M.I. Rabinovich, *Sov. Phys. JETP* 41 (1986) 157.
- [16] N.B. Tufillaro, R. Ramshankar, J.P. Gollub, *Phys. Rev. Lett.* 62 (1989) 422.
- [17] S. Ciliberto, S. Douady, S. Fauve, *Europhys. Lett.* 15 (1991) 23.
- [18] B. Christiansen, P. Alstrom, M. Levinsen, *Phys. Rev. Lett.* 68 (1992) 2157.
- [19] E. Bosch, W. van der Water, *Phys. Rev. Lett.* 70 (1993) 3420.
- [20] W.S. Edwards, S. Fauve, *Phys. Rev. E* 47 (1993) 788.
- [21] W.S. Edwards, S. Fauve, *J. Fluid Mech.* 278 (1994) 123.
- [22] J. Bechhoefer, V. Ego, S. Manneville, B. Johnson, *J. Fluid Mech.* 288 (1995) 325.
- [23] O. Lioubashevski, J. Fineberg, L.S. Tuckerman, *Phys. Rev. E* 55 (1997) 3832.
- [24] J. Wu, R. Keolian, I. Rudnick, *Phys. Rev. Lett.* 52 (1984) 1421.
- [25] A. Larraza, S. Putterman, *J. Fluid Mech.* 148 (1984) 443.
- [26] J.W. Miles, *J. Fluid Mech.* 148 (1984) 451.
- [27] K. Kumar, L.S. Tuckerman, *J. Fluid Mech.* 279 (1994) 49.